HHS Public Access

Author manuscript

Cell Rep. Author manuscript; available in PMC 2019 February 12.

Published in final edited form as:

Cell Rep. 2018 December 04; 25(10): 2766–2774.e3. doi:10.1016/j.celrep.2018.11.020.

CMV Primes Functional Alternative Signaling in Adaptive Δg NK Cells but Is Subverted by Lentivirus Infection in Rhesus Macaques

Spandan V. Shah[1], **Cordelia Manickam**[1], **Daniel R. Ram**[1], **Kyle Kroll**[1], **Hannah Itell**[2], **Sallie R. Permar**[2], **Dan H. Barouch**[1,3], **Nichole R. Klatt**[4,5], and **R. Keith Reeves**[1,3,6,*]

[1]Center for Virology and Vaccine Research, Beth Israel Deaconess Medical Center, Harvard Medical School, Boston, MA 02115, USA

[2]Human Vaccine Institute, Duke University Medical Center, Durham, NC 27710, USA

[3]Ragon Institute of Massachusetts General Hospital, MIT, and Harvard, Cambridge, MA 02139, USA

[4]Department of Pharmaceutics, Washington National Primate Research Center, University of Washington, Seattle, WA 98195, USA

[5]Department of Pediatrics, University of Miami, Miami, FL 33136, USA

[6]Lead Contact

SUMMARY

Despite burgeoning evidence demonstrating the adaptive properties of natural killer (NK) cells, mechanistic data explaining these phenomena are lacking. Following antibody sensitization, NK cells lacking the Fc receptor (FcR) signaling chain (Δg) acquire adaptive features, including robust proliferation, multi-functionality, rapid killing, and mobilization to sites of virus exposure. Using the rhesus macaque model, we demonstrate the systemic distribution of Δg NK cells expressing memory features, including downregulated Helios and Eomes. Furthermore, we find that Δg NK cells abandon typical γ-chain/Syk in lieu of CD3ζ-Zap70 signaling. FCγRIIIa (CD16) density, mucosal homing, and function are all coupled to this alternate signaling, which in itself requires priming by rhesus cytomegalovirus (rhCMV). Simian immunodeficiency virus (SIV) infections further expand gut-homing adaptive NK cells but result in pathogenic suppression of CD3ζ-Zap70 signaling and function. Herein, we provide a mechanism of virus-dependent alternative signaling that may explain the acquisition of adaptive features by primate NK cells and could be targeted for future vaccine or curative therapies.

*Correspondence: rreeves@bidmc.harvard.edu.

AUTHOR CONTRIBUTIONS

R.K.R. designed the studies. S.V.S., C.M., D.R.R., H.I., and K.K. conducted assays. S.R.P., D.H.B., and N.R.K. contributed valuable analyses, samples, and data interpretation. S.V.S. and R.K.R. wrote the paper with the assistance of all the co-authors.

SUPPLEMENTAL INFORMATION

Supplemental Information includes six figures and can be found with this article online at https://doi.org/10.1016/j.celrep.2018.11.020.

DECLARATION OF INTERESTS

The authors declare no competing financial interests.

Graphical Abstract

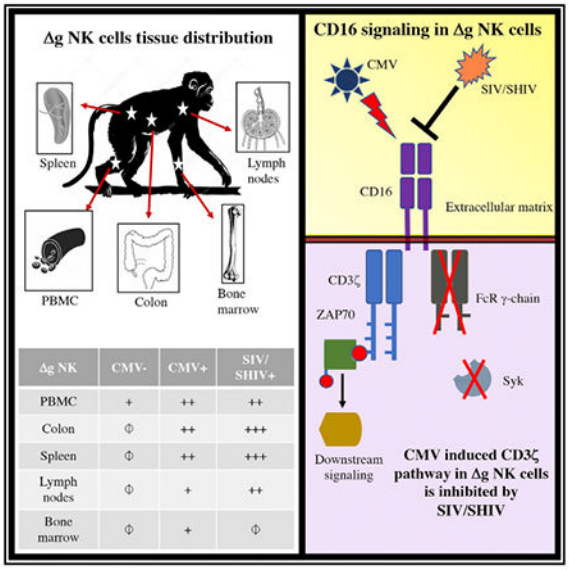

In Brief

Gamma-chain-deficient adaptive NK cells are robust mediators of antiviral immunity via ADCC. Shah et al. demonstrate using macaque models that acquisition of these features requires previous priming with CMV infection and involves alternative signaling via CD3zeta but is actively suppressed by lentivirus infection.

INTRODUCTION

Classically considered a part of the innate system, natural killer (NK) cells represent a heterogeneous cell population integrating activating and inhibiting receptors to mediate killing and cytokine-based modulation of tumor and virus-infected cells. One major contribution of the NK cell repertoire is serving as the effector cell against targets bound by antibody in antibody-dependent cell-mediated cytotoxicity (ADCC). During HIV and simian immunodeficiency virus (SIV) infections, NK cells contribute to the control of virus replication and disease progression through multiple mechanisms and specifically elicit robust ADCC responses (Alter et al., 2011; Alter et al., 2007; Bostik et al., 2009; Fehniger et al., 1998; Fogli et al., 2008; He et al., 2013; Parsons et al., 2012; Reeves et al., 2010b; Ward et al., 2007). Indeed, ADCC has been implicated in superior antiviral activities in HIV-1 “elite controllers” (Lambotte et al., 2009; Wren et al., 2013) and may have contributed to protective effects elicited by non-neutralizing antibodies in the RV144 Thai trial (Haynes et al., 2012).

Immune experience significantly influences diversity in the NK cell receptor repertoire (Strauss-Albee et al., 2015), and although few viruses are known to infect NK cells directly, viral infections can drive diversification, activation, and dysfunction of NK cells *in vivo* (Brandstadter and Yang, 2011; Ma et al., 2016). CMV infection tunes NK cell education and expansion of specific NK cell subsets (Béziat et al., 2013), and some of the first

characterizations of adaptive NK cells were found in murine CMV infection, with analogous adaptive expansion found in human cytomegalovirus (HCMV) (Dokun et al., 2001; Hammer and Romagnani, 2017; Hendricks et al., 2014; Lopez-Vergès et al., 2011; Robbins et al., 2004; Sun et al., 2009). Multiple studies confirmed that murine NK cells mediate recall against non-CMV antigens (Gillard et al., 2011; Majewska-Szczepanik et al., 2013; O'Leary et al., 2006; Paust et al., 2009), and memory NK cell responses subsequently have been demonstrated against multiple pathogens in mice and humans (Paust et al., 2017). Evidence of memory NK cells was shown in rhesus macaques by our laboratory (Reeves et al., 2015). In addition to the description of antigen-specific NK cells, recent evidence has also identified a subpopulation of memory-like or adaptive NK cells that are exquisite effector cells when granted specificity through antibody binding. These cells first described in humans in 2012 by Zhang et al. (Hwang et al., 2012) express high levels of FcγR (including CD16) but lack the γ-signaling chain. So-called g– or Δg NK cells are found at low frequencies in all individuals but expand in CMV-seropositive persons. Following initial antibody binding, these cells may be epigenetically modified but become long-lived and capable of recall-like responses (Lee et al., 2015; Schlums et al., 2015). Recently, Δg NK cells have been shown to be increased 7-fold in HIV-infected persons and are associated with enhanced ADCC against HIV antigens (Zhou et al., 2015). Although these γ-chain deficient, Syk-deficient NK cells have been reported in humans, such an observation has not been made in any effector sites or in macaques or mice, leaving a critical animal model lacking for the study of these cells. Most importantly, the mechanisms that promote enhanced adaptive function by Δg and other memory and adaptive NK cell populations, as well as the role of CMV in this innate priming, remain largely unexplored.

RESULTS

Δg NK Cells Comprise a Distinct Subset of Primate NK Cells

We first identified a distinct circulating population of Syk^{lo} γ-chain$^{-/lo}$ NK cells in rhesus cytomegalovirus (rhCMV)-positive macaques (Figure 1A) among standardly defined macaque CD3^{-}CD14^{-}CD20^{-}HLA-DR^{dim} NKG2A/C+ NK cells (Reeves et al., 2010b; Shang et al., 2014; Takahashi et al., 2014) and confirmed co-expression of other NK cell-related markers, such as NKp46 and CD8α (Figure 1B; Figures S1A and S1B). Δg NK cells expressed reduced levels of the inhibitory receptor Siglec-7 (Figure S1C), suggesting a more basal activation state, and also had downregulated expression of the NK cell transcription factors Helios and Eomes compared with conventional NK (cNK) cells (Figure 1B; Figures S1D and S1E), likely indicative of a disparate developmental program or epigenetic modification (Lee et al., 2015). Δg NK cells had a higher frequency of CD16+ subpopulations (Figure 1C; Figure S1F), higher Fas (CD95) expression (Figures S2A and S2B), and increased cytotoxic arming with Granzyme B than the cNK cells (Figures S2C and S2D). Multidimensional t-distributed stochastic neighbor embedding (*t*-SNE) analyses of flow cytometric markers confirmed that although, as expected, there is significant phenotypic overlap with cNK, Δg NK cells segregate and are distinct (Figure 1D; Figure S3). Principal-component analysis (PCA) revealed a similar disparate relationship between Δg and cNK cells, most heavily influenced by γ-chain and Syk (Figure 1E). Collectively,

these data confirmed the identification of a highly distinct functionally robust and transcriptionally modified Δg NK cell population.

rhCMV Expands and Primes Adaptive Δg NK Cells

Initial observations have suggested that the expansion of Δg and other memory and adaptive NK cells is linked to CMV infection (Lee et al., 2015; Sun et al., 2009). To validate these findings, we quantified Δg NK cells in cohorts of rhCMV-uninfected and rhCMV-infected rhesus macaques. Frequencies of Δg among total NK cells were significantly higher than cNK cells (medians, 8.5% and 17.4%, CMV− and CMV+, respectively) (Figure 2A), but most striking was the one-log expansion in absolute Δg NK cells in circulation (Figure 2B). Δg NK cells from rhCMV-infected animals also had significantly reduced Helios and upregulated CD16 expression (Figures 2C and 2D), suggesting that not only does rhCMV induce an expansion of the adaptive Δg NK cell population but also regulates transcriptional and phenotypic changes. Indeed, Δg NK cells from rhCMV-uninfected and rhCMV-infected macaques clustered completely independently by *t*-SNE (Figure 2E) and, importantly, were tightly associated with rhCMV-specific immunoglobulin G (IgG) levels as a surrogate indicator of virus replication (Figure 2F). The disparate CD16 expression (Figure 2; Figure S1F) also suggests these cells may have enhanced antibody binding and thereby improve functional recognition.

Δg NK Cells Are Found Systemically but Have Disparate Tissue-Homing Patterns

Previous evaluations of adaptive NK cells have focused exclusively on characterizing these cells in human blood or culture systems, leaving a significant deficit as to whether or not this population could exist in meaningful effector sites. To address this deficit, we quantified Δg NK cells in multiple tissues and found them systemically distributed among spleen, bone marrow, multiple lymph node sites, and colonic mucosae (Figure 3A; Figure S6). Although found systemically, Δg NK cells were notably more enriched (Mann-Whitney U, $p = 0.02$) in colonic tissue NK cells (median, 8.1%; range, 4.4 to 11.9%) than lymph node NK cells (median, 4.3%; range, 1.6 to 7.6%) from normal rhCMV-infected animals (Figure S6). Differences in homing properties between circulating Δg and cNK cells helped to clarify this distribution (Figure 3B). Both CCR7 and CD62L, lymph node homing markers, were downregulated in Δg NK cells, whereas gut-homing α4β7 was 100% increased in circulating Δg cells compared with matched cNK cells (Figures 3C–3E). Notably, these homing properties were not different when stratified by rhCMV status and, thus, may not be part of the NK cell repertoire that is impacted by CMV priming. We also analyzed whether these same differences were observed in tissue-resident NK cells and indeed found that Δg NK cells exhibited lower CCR7 and CD62L than their cNK cell counterparts in lymph nodes (Figures 3F and 3G). Furthermore, α4β7 was significantly upregulated in Δg NK cells in colonic tissue (Figure 3H), suggesting that these cells not only may preferentially home to the mucosae but also may be retained there. Altogether, these data demonstrate the systemic distribution of Δg NK cells but indicate that this NK cell population may preferentially survey effector sites, such as the gut, and not traffic through lymph nodes at the same frequency as cNK cells.

SIV Infection Systemically Expands Δg NK Cells and Induces Mucosal Homing

Although CMV is a primary factor in the expansion and priming of Δg NK cells, the impact of other viruses remains poorly explored. In a large cohort of rhCMV-infected macaques that were experimentally challenged and chronically infected with SIVmac251 or SHIV162p3, we found slight but not statistically significant increases in frequencies and numbers of Δg NK cells in circulation compared with rhCMV-infected/SIVmac251/SHIV162p3-naive animals (Figures 2A, 2B, 4A, and 4B). Despite little change in blood, significant 2- to 5-fold increases of Δg NK cells were found in the colon, lymph nodes, and spleen, indicating that SIVmac251/SHIV162p3 infection may preferentially induce expansion at effector sites (Figure 4C). Δg NK cell numbers are closely associated with rhCMV-specific IgG levels (Figure 4E) rather than SIV viral loads (Figure 4F), suggesting that numerical expansion is likely caused by increased rhCMV replication, a known phenomenon in HIV and SIV infections (Gianella and Letendre, 2016), whereas mucosal redistribution may be due to SIV infection. Indeed, the most robust increase was found in the colonic tissue of SIVmac251/SHIV162p3-infected macaques, and gut-homing α4β7, already preferentially expressed on Δg NK cells, is further significantly upregulated in circulating cells (Figure 4D). Collectively, these data demonstrate that rhCMV-primed Δg NK cells are modified by SIV infection to home to mucosal and effector tissues.

Δg NK Cell Function Requires rhCMV Priming but Is Dysregulated in SIV Infection

Δg NK cells may have disparate functional profiles from cNK cells and have previously been shown to have recall-like capabilities (Lee et al., 2015). Our data indicated that Δg NK cells have increased cytotoxic arming (Figure S2), and here, we tested the impact of rhCMV infection in rhesus macaques on not only cytotoxic function but also cytokine production by using a modified ADCC assay (Figure 5). Not surprisingly, Δg NK cells had similar upregulation of CD107a (as a surrogate marker for cytotoxicity) and tumor necrosis factor alpha (TNF-α), interferon gamma (IFN-γ), and macrophage inflammatory protein 1 beta (MIP-1β) production compared with cNK cells in rhCMV-infected animals. However, in rhCMV-uninfected macaques, Δg NK cells were almost completely non-responsive to antibody-target cell stimulation. These data confirmed and expanded previous observations that although cNK cells are functionally competent irrespective of CMV serostatus, Δg NK cells require CMV infection not only for numerical expansion but also to gain function.

We next evaluated the effects of chronic SIV infection on both cNK and Δg NK cells.

Other than CD107a, cNK cells had reduced functional capacity for all functions compared with rhCMV-infected/SIV-naive animals. Δg NK cells had even further suppressed functions, indicating that all NK cells show signs of ADCC dysfunction in SIV infection, this population may be disproportionately impacted.

Δg NK Cells Use Alternative Signaling Induced by rhCMV Priming

The dramatic differences in CMV-driven function between Δg and cNK cells have been previously attributed, at least in part, to epigenetic modification (Lee et al., 2015). However, no clear mechanistic explanation has been elucidated for these and other types of memory and adaptive NK cells. Furthermore, because Δg NK cells lack the traditional γ-chain/Syk

signaling, enhanced function in this cell population is counter-intuitive, and we hypothesized that Δg NK cells might switch to an alternative signaling pathway not typically used by CD16 binding. Indeed, we found that in lieu of the γ-chain (Figure 1), Δg NK cells had up-regulated expression of CD3ζ and its adaptor molecule ZAP70, which can also alternatively mediate CD16-dependent signaling, as well as DAP12, all primed by rhCMV status (Figures 6A–6C). Next, we evaluated levels of active signaling of these pathways, as measured by phosphorylation on activation sites. Not surprisingly, we confirmed that cNK cells, regardless of CMV status, use the Syk pathway, as indicated by activated pSyk, whereas Δg NK cells do not (Figures S4A and S4B). Phosphorylation of CD3ζ was greatest in rhCMV-infected animals overall, indicating it can be used by any NK cell, but was only present in Δg NK cells after rhCMV infection (Figures 6D and 6E). Furthermore, we found that phosphorylation of the CD3ζ adaptor Zap70 is significantly greater in Δg than cNK cells (Figures S5A and S5B). These data demonstrate that adaptive Δg NK cell function relies at least partly on CD3ζ-Zap70 signaling but is also tightly coupled to previous rhCMV infection.

In identical assays, SIV-infected animals (as well as rhCMV-infected animals) showed evidence of extremely dysregulated signaling pathways. Expression patterns of CD3ζ were similar, but ZAP70 and DAP12 were downregulated (Figures 6B and 6C). Even in cNK cells, the levels of Syk phosphorylation (the traditional pathway for these cells) were dramatically lower in SIV-infected animals than both rhCMV-uninfected and rhCMV-infected samples (Figures S4A and S4B), but most notably for Δg NK cells, alternative CD3ζ phosphorylation was near the limit of detection (Figure 6E). Taken together with the fact that phenotypically Δg NK cells cluster completely independently in SIV-infected and SIV-naive animals, these data may explain the well-described dysfunction of NK cells in HIV and SIV infections (Figure 5) (Alter et al., 2005; Reeves et al., 2010b) and indicate an active suppression of the adaptive Δg NK cells.

DISCUSSION

The studies herein provide some of the most robust insights into the combinatorial mechanisms of innate priming that explain the functional potency of Fc receptor (FcR)-bearing Δg adaptive NK cells. Specifically, our data elaborate on two phenomena: (1) Δg NK cells are rare and non-functional prior to CMV exposure but after CMV priming, expand numerically, functionally, and become active due to an alternative signaling switch to the CD3ζ-Zap70 pathway; and (2) dysfunction of CD16-mediated signaling in both cNK and Δg NK cells occurs in lentivirus infection and can be explained by abrogation of both γ-chain/Syk and CD3ζ-Zap70 signaling.

Although Δg NK cells have been described in human subjects (Lee et al., 2015), the fully functional niche, as well as distribution in tissues and species, has remained unclear. Others and we have now shown that Δg NK cells can produce cytokines as well as be simultaneously cytotoxic, and previous research indicates that epigenetic modification following antibody-antigen exposure drives more robust functionality (Lee et al., 2015). However, the differences we observed in the transcriptional regulation and the specific expansion of Δg cells but not cNK cells in rhCMV-infected animals suggests they could also

represent an independent lineage of NK cells, as has been previously suggested for other memory NK cell subpopulations (Paust et al., 2017). Regardless, both numerical and functional expansions depend on rhCMV priming, as Δg NK cells were essentially non-functional in rhCMV-uninfected subjects (Figures 2 and 5). Indeed, rhCMV status induced multifunctional responses, but also, the upregulation of Granzyme B and Fas are further indicative of an active priming of multiple cytotoxic mechanisms. rhCMV also induced a downregulation of inhibitory molecules, such as Siglec-7, but an upregulation of CD16. FcR like CD16 are typically recycled relatively quickly on the surface of NK cells by a series of enzymes, including ADAM17 (TACE), the inhibition of which has shown promise as an anti-tumor therapy (Romee et al., 2013). Future studies will need to determine if this type of mechanism could be specifically inhibited by CMV or is less active in Δg NK cells, but also further emphasizes that increased FcR stability and reduced inhibitory molecule expression promote enhanced functional activity. Another unexpected feature of Δg NK cells was the reduced expression of lymph node-homing molecules in lieu of the upregulation of gut-homing α4β7. Retinoic acid is a primary regulator of cell surface α4β7 expression (Mora et al., 2003) and has a reciprocal relationship with CMV (Ghazal et al., 1992), so increased expression may be a direct consequence of ongoing rhCMV replication. Regardless, this altered expression pattern could explain, at least in part, the enrichment of these cells in the mucosae and suggests they may have a more active role in surveillance of effector sites.

One component of our study was to address the effects of lentivirus infection on systemic numbers and functions of Δg NK cells and in an animal model. A recent study indicated that Δg NK cells expand numerically in HIV infection (Zhou et al., 2015), but our observations further clarify that this is most likely associated with rhCMV replication rather than HIV or SIV. However, we did find that in chronic SIV infection, Δg NK cells upregulated α4β7 and increased homing to colonic tissue and other effector sites (Figure 4). Perturbed retinoid metabolism in infection (Loignon et al., 2012) is a putative source of increased imprinting of α4β7 on Δg NK cell mucosal homing, and we and others have previously found this may be a generalized NK cell phenomenon in SIV infection (Reeves et al., 2010a). Consistent with previous observations for cNK cells in HIV infection (Alter et al., 2005), SIV also caused a significant dysregulation of Δg NK cell functionality that could be due to anergy and exhaustion (Schafer et al., 2015), but, as discussed below, this is most likely due to dysregulated signaling. Collectively, data from our study and others indicate that HIV and SIV may not influence the expansion or priming of the Δg NK cell population per se but can indirectly have major impacts on trafficking and function.

Another important observation in our study is that Δg NK cells in rhesus macaques, and similarly in humans (Liu et al., 2016), do not use the γ-chain/Syk CD16 signaling pathway but rather use CD3ζ/Zap70 signaling and only after CMV priming. Although the need for CD16 to signal through γ-chain or CD3ζ molecules is well established, whether the recruitment of either molecule is inherent to a specific downstream function is less clear (Lanier, 2008; O'Shea et al., 1991; Vivier et al., 1992; Wirthmueller et al., 1992). Homodimers of γ-chain are preferentially expressed in NK cells and cytotoxic T cells, suggesting that this is the preferential arrangement for cytotoxic functions, particularly in mice, but heterodimers of CD3ζ and γ-chain may be the more common pathway for ADCC in humans (Vivier et al., 1991a; Vivier et al., 1991b). This concept is clearly reflected in our

data whereby cNK cells assemble the γ-chain/Syk complex but also express comparable levels of CD3ζ, suggesting that macaque cNK cells are likely using a heterodimeric complex. However, in Δg NK cells, a CMV-associated lack of γ-chain leads to a less common CD3ζ homodimeric-ZAP70 complex to induce much more robust FcR-mediated effector responses (Figure 5). These data highlight the underappreciated signaling heterogeneity that may occur in memory and adaptive NK cell subsets, and the overall lack of CD3ζ signaling may explain, in part, why Δg NK cells do not appear to exist in mice, further underscoring the need for an animal model, such as rhesus macaques. Beyond rhCMV-priming of Δg NK cells, the most dramatic signaling changes were observed in SIV-infected animals (Figure 6). Activation of both γ-chain and CD3ζ pathways were dramatically suppressed, which likely explains the functional dysregulation of both Δg and cNK cells in HIV and SIV infections (Figure 5)(Alter et al., 2005). These data also raise the alternative hypothesis that other molecules and signaling pathways may be recruited in NK cells during HIV and SIV infection or that a different immunoreceptor tyrosine-based activation motif (ITAM) of CD3ζ (other than the typical third ITAM, Y142) may be phosphorylated. However, the fact that DAP12, associated with NKG2D signaling (Garrity et al., 2005), is also downregulated in SIV infection (Figure 5) suggests this is a global suppression of active NK cell signaling and will need significant additional studies to elucidate the full mechanisms. Overall, our data indicate that Δg NK cells recruit specific signaling machinery as part of an alternative repertoire to mount a robust virus-tuned response but can be actively inhibited by lentivirus infection.

Altogether, we present herein a demonstration of adaptive Δg NK cells in tissues, delineate a primary mechanism of functional potency, explain in part NK cell functional dysregulation in SIV infection, and importantly solidify a tangible animal model to study this cell population. The functional potency of Δg NK cells indicates they could be very attractive targets for antibody-based therapeutics and vaccine modalities against HIV and other pathogens. Further research will be needed to evaluate the protective efficacy of these responses and if they could be experimentally modulated or expanded outside of natural rhCMV infection or restored in SIV infection.

STAR★METHODS

CONTACT FOR REAGENT AND RESOURCE SHARING

Further information and requests for resources and reagents should be directed to and will be fulfilled by the Lead Contact, R. Keith Reeves (rreeves@bidmc.harvard.edu).

EXPERIMENTAL MODEL AND SUBJECT DETAILS

Macaques—A total of seventy male and female Indian origin rhesus macaques (*Macaca mulatta*) were used in various components of this study: 28 specific pathogen-free rhCMV-uninfected (< 1 mg/ml anti-rhCMV IgG); 14 rhCMV-infected but otherwise experimentally naive; 8 chronically infected with SHIVsf162p3, and 20 chronically SIVmac239/251-infected macaques. All animals were randomized to infection groups without specific exclusion and technical staff were blinded to groupings at the time of analyses. All groups contained comparable numbers of males and females and no significant differences in the

data were observed based on gender, and ranged in age from 1.7 to 11.6 years at the time of study. All animals were healthy based on veterinary examination, and SIV and SHIV-infected macaques were exhibiting clinical signs of AIDS at the time of analysis. Animals were cared for according to the guidelines of the local Institutional Animal Care and Use Committee (IACUC). Animals were euthanized in order to collect tissues for analyses.

METHOD DETAILS

rhCMV antibody titers and SIV viral loads—Total rhCMV-specific IgG levels were measured in cell free plasma (Nelson et al., 2017), and SIV viral loads were measured by RT-PCR with RNA purified by the phenol-chloroform technique. Viral RNA was isolated from plasma using RNA extraction kit (QIAGEN, Germantown, MD) and manufacturer's protocol was followed. Quantified RNA was used for RT-PCR against a conserved region of *gag* using gene-specific primers (Whitney et al., 2014). In the first step, RNA was reverse-transcribed followed by treatment with RNaseH for 20 min at 37°C. Next, cDNA was amplified using 7300 ABI Real-Time PCR system (applied Biosystems) according to the manufacturer's protocol.

Blood and tissue collection and processing—EDTA-treated venous blood was also collected at various time points and mononuclear cells were isolated using Ficoll-Paque™ (GE Healthcare, Waukesha, WI). Spleen, lymph nodes (LN), bulk bone marrow (BM) and colon were collected and mononuclear cells were isolated using procedures that have been previously described in our laboratory (Reeves et al., 2010b; Reeves et al., 2015). Single-cell suspensions were prepared by mechanical disruption using syringe tops and 70 μm strainers (ThermoFisher Scientific, Waltham, DA). Suspended cells were either loaded on Percoll (colon) or Ficoll-Paque™ (blood, BM, liver spleen, and LN) solutions to separate cells using density-gradient centrifugation technique. Mononuclear cells were isolated from the interface of a 30%–60% discontinuous Percoll gradient or Ficoll-Paque™ according to manufacturers' suggested protocols. A hypotonic ammonium chloride solution (ACK, ThermoFisher Scientific, Waltham, DA) was used to lyse contaminating red blood cells. Cells were either immediately cultured or cryopreserved in freezing media (90% FBS, 10% DMSO) and stored in liquid nitrogen vapor. All procedures were conducted in a biosafety level 2 facility.

Surface flow cytometry—Fluorochrome-conjugated antibodies were purchased from BD Biosciences (San Jose, CA), ThermoFisher Scientific (Waltham, MA), Beckman-Coulter (Indianapolis, IN) and Cell Signaling Technology (Danvers, MA). Q-Prep (Beckman-Coulter) on PBMC was used for surface staining or intracellular staining. Antibodies used are listed in the Key Resources Table. Before antibody staining, cells were stained with Aqua Live/Dead stain (Invitrogen, Carlsbad, CA) for 30 minutes at room temperature in the dark followed by a wash step (PBS + 2% FBS). Data acquisitions were performed on an LSR II (BD Biosciences), and FlowJo software (version 9.9.4, Tree Star, Ashland, OR) was used for all analyses.

Intracellular staining—All intracellular staining was performed using Fix & Perm buffer kit (ThermoFisher Scientific, Waltham, MA). Briefly, cells were thawed at 37°C water bath

and washed once before incubating for 6 hours at 37°C with PMA (0.05 μg/reaction) and Ionomycin (1 μg/reaction), followed by staining with surface antibodies. Then cells were fixed with Perm Buffer A followed by incubation with intracellular antibodies mixed with Perm Buffer B according to manufacturer's protocol. Cells were washed twice and fixed again with PFA before data acquisition.

Phospho-flow—BD Perm buffer III (BD Biosciences, La Jolla, CA) was used for phospho-flow analyses according to the manufacturers' protocols. Briefly, cells were opsonized with anti-human CD16 (BD Biosciences, clone 3G8, La Jolla, CA) followed by cross-linking with secondary goat-anti-mouse F(ab)'2, (Jackson ImmunoResearch Laboratories, West Grove, PA). Reactions were immediately stopped after 2.5 minutes (experimentally determined, data not shown) with equal volumes of Fix Buffer I (BD Biosciences, La Jolla, CA). After washing, unused/ unoccupied sites of the secondary antibody were blocked with normal mouse serum (ThermoFisher) for 10 minutes at room temperature. Fixation was followed by surface stain, permeabilization with Perm Buffer III for 30 minutes on ice, followed by intracellular staining at room temperature according to the manufacturer's protocol.

Multiparametric analysis—FCS files were imported into FlowJo v9.9.6 and manual gating analysis was used to select live NK cells as defined in Figure 1. NK cell population data were exported and multiparametric analyses were performed using the Cyt program (Amir et al., 2013). Briefly, data were loaded into Cyt, transformed, concatenated and Barnes-Hut *t*-distributed stochastic neighboring embedding (bh-SNE) and Principal Component Analysis (PCA) were performed. Manual gating was used to overlay color on target populations.

Antibody dependent cell cytotoxicity—Isolated fresh or frozen PBMCs were rested overnight, counted and co-cultured for 6 hours at a 25:1 effector to target ratio with CEM.NKR target cells in the presence or absence of 10 μg/mL rhesusized anti-human CD4. Unbound rhesusized anti-human CD4 was removed from the culture media via wash steps prior to the co-culture. Anti-CD4 antibody concentrations and effector to target ratio were determined from prior titration experiments (data not shown). Brefeldin A, monensin, and CD107a, were added at the start of incubation. After incubation cells were stained for both surface and intracellular proteins using antibodies described above.

QUANTIFICATION AND STATISTICAL ANALYSIS

Statistical analysis—All statistical and graphic analyses were conducted with GraphPad Prism 7.0 software (GraphPad Software, La Jolla, CA). Nonparametric Mann-Whitney *U*-tests, Wilcoxon Matched Pairs test, Student's t tests, and Spearman's correlations were used where indicated, and a *P value* of < 0.05 (by two-tailed test) was considered statistically significant. Nonparametric tests were used because data were determined not to be normally distributed as is anticipated for outbred animal studies.

DATA AND SOFTWARE AVALAIBILITY

All data shown in Figures and Supplemental Figures show raw values and data points indicate individual animals. All data generated and analyzed in this study are available from the corresponding author upon reasonable request.

Supplementary Material

Refer to Web version on PubMed Central for supplementary material.

ACKNOWLEDGMENTS

This work was supported by NIH grants R01 AI120828, P01 AI120756, and R01 DE026014 (to R.K.R.); the Harvard Center for AIDS Research grant P30 AI060354 and colony grants U42 OD024282, U42 OD010568, and P51 OD011104; and by the Ragon Institute of MGH, MIT, and Harvard (to D.H.B.). The authors thank Michelle Lifton, Dr. James Whitney, and Dr. Soyon Lim for their technical assistance.

REFERENCES

Alter G, Teigen N, Davis BT, Addo MM, Suscovich TJ, Waring MT, Streeck H, Johnston MN, Staller KD, Zaman MT, et al. (2005). Sequential deregulation of NK cell subset distribution and function starting in acute HIV-1 infection. Blood 106, 3366–3369. [PubMed: 16002429]

Alter G, Teigen N, Ahern R, Streeck H, Meier A, Rosenberg ES, and Altfeld M (2007). Evolution of innate and adaptive effector cell functions during acute HIV-1 infection. J. Infect. Dis 195, 1452–1460. [PubMed: 17436225]

Alter G, Heckerman D, Schneidewind A, Fadda L, Kadie CM, Carlson JM, Oniangue-Ndza C, Martin M, Li B, Khakoo SI, et al. (2011). HIV-1 adaptation to NK-cell-mediated immune pressure. Nature 476, 96–100. [PubMed: 21814282]

Amir E, Davis KL, Tadmor MD, Simonds EF, Levine JH, Bendall SC, Shenfeld DK, Krishnaswamy S, Nolan GP, and Peer D (2013). viSNE enables visualization of high dimensional single-cell data and reveals phenotypic heterogeneity of leukemia. Nat. Biotechnol 31, 545–552. [PubMed: 23685480]

Béziat V, Liu LL, Malmberg JA, Ivarsson MA, Sohlberg E, Björklund AT, Retière C, Sverremark-Ekström E, Traherne J, Ljungman P, et al. (2013). NK cell responses to cytomegalovirus infection lead to stable imprints in the human KIR repertoire and involve activating KIRs. Blood 121, 2678–2688. [PubMed: 23325834]

Bostik P, Kobkitjaroen J, Tang W, Villinger F, Pereira LE, Little DM, Stephenson ST, Bouzyk M, and Ansari AA (2009). Decreased NK cell frequency and function is associated with increased risk of KIR3DL allele polymorphism in simian immunodeficiency virus-infected rhesus macaques with high viral loads. J. Immunol 182, 3638–3649. [PubMed: 19265142]

Brandstadter JD, and Yang Y (2011). Natural killer cell responses to viral infection. J. Innate Immun 3, 274–279. [PubMed: 21411975]

Dokun AO, Kim S, Smith HR, Kang HS, Chu DT, and Yokoyama WM (2001). Specific and nonspecific NK cell activation during virus infection. Nat. Immunol 2, 951–956. [PubMed: 11550009]

Fehniger TA, Herbein G, Yu H, Para MI, Bernstein ZP, O'Brien WA, and Caligiuri MA (1998). Natural killer cells from HIV-1 + patients produce C-C chemokines and inhibit HIV-1 infection. J. Immunol 161, 6433–6438. [PubMed: 9834136]

Fogli M, Mavilio D, Brunetta E, Varchetta S, Ata K, Roby G, Kovacs C, Follmann D, Pende D, Ward J, et al. (2008). Lysis of endogenously infected CD4+ T cell blasts by rIL-2 activated autologous natural killer cells from HIV-infected viremic individuals. PLoS Pathog 4, e1000101. [PubMed: 18617991]

Garrity D, Call ME, Feng J, and Wucherpfennig KW (2005). The activating NKG2D receptor assembles in the membrane with two signaling dimers into a hexameric structure. Proc. Natl. Acad. Sci. USA 102, 7641–7646. [PubMed: 15894612]

Ghazal P, DeMattei C, Giulietti E, Kliewer SA, Umesono K, and Evans RM (1992). Retinoic acid receptors initiate induction of the cytomegalovirus enhancer in embryonal cells. Proc. Natl. Acad. Sci. USA 89, 7630–7634. [PubMed: 1323848]

Gianella S, and Letendre S (2016). Cytomegalovirus and HIV: a dangerous pas de deux. J. Infect. Dis 214, S67–S74. [PubMed: 27625433]

Gillard GO, Bivas-Benita M, Hovav AH, Grandpre LE, Panas MW, Seaman MS, Haynes BF, and Letvin NL (2011). Thy1+ NK [corrected] cells from vaccinia virus-primed mice confer protection against vaccinia virus challenge in the absence of adaptive lymphocytes. PLoS Pathog 7, e1002141. [PubMed: 21829360]

Hammer Q, and Romagnani C. (2017). About training and memory: NK-cell adaptation to viral infections. Adv. Immunol 133, 171–207. [PubMed: 28215279]

Haynes BF, Gilbert PB, McElrath MJ, Zolla-Pazner S, Tomaras GD, Alam SM, Evans DT, Montefiori DC, Karnasuta C, Sutthent R, et al. (2012). Immune-correlates analysis of an HIV-1 vaccine efficacy trial. N. Engl. J. Med 366, 1275–1286. [PubMed: 22475592]

He X, Li D, Luo Z, Liang H, Peng H, Zhao Y, Wang N, Liu D, Qin C, Wei Q, et al. (2013). Compromised NK cell-mediated antibody-dependent cellular cytotoxicity in chronic SIV/SHIV infection. PLoS ONE 8, e56309. [PubMed: 23424655]

Hendricks DW, Balfour HH, Jr., Dunmire SK, Schmeling DO, Hogquist KA, and Lanier LL (2014). Cutting edge: NKG2C(hi)CD57+ NK cells respond specifically to acute infection with cytomegalovirus and not Epstein-Barrvirus. J. Immunol 192, 4492–4496. [PubMed: 24740502]

Hwang I, Zhang T, Scott JM, Kim AR, Lee T, Kakarla T, Kim A, Sunwoo JB, and Kim S (2012). Identification of human NK cells that are deficient for signaling adaptor FcRγ and specialized for antibody-dependent immune functions. Int. Immunol 24, 793–802. [PubMed: 22962434]

Lambotte O, Ferrari G, Moog C, Yates NL, Liao HX, Parks RJ, Hicks CB, Owzar K, Tomaras GD, Montefiori DC, et al. (2009). Heterogeneous neutralizing antibody and antibody-dependent cell cytotoxicity responses in HIV-1 elite controllers. AIDS 23, 897–906. [PubMed: 19414990]

Lanier LL (2008). Up on the tightrope: natural killer cell activation and inhibition. Nat. Immunol 9, 495–502. [PubMed: 18425106]

Lee J, Zhang T, Hwang I, Kim A, Nitschke L, Kim M, Scott JM, Kamimura Y, Lanier LL, and Kim S (2015). Epigenetic modification and antibody-dependent expansion of memory-like NK cells in human cytomegalovirus-infected individuals. Immunity 42, 431–442. [PubMed: 25786175]

Liu LL, Landskron J, Ask EH, Enqvist M, Sohlberg E, Traherne JA, Hammer Q, Goodridge JP, Larsson S, Jayaraman J, et al. (2016). Critical role of CD2 co-stimulation in adaptive natural killer cell responses revealed in NKG2C-deficient humans. Cell Rep 15, 1088–1099. [PubMed: 27117418]

Loignon M, Brodeur H, Deschênes S, Phaneuf D, Bhat PV, and Toma E (2012). Combination antiretroviral therapy and chronic HIV infection affect serum retinoid concentrations: longitudinal and cross-sectional assessments. AIDS Res. Ther. 9, 3. [PubMed: 22296672]

Lopez-Vergès S, Milush JM, Schwartz BS, Pando MJ, Jarjoura J, York VA, Houchins JP, Miller S, Kang SM, Norris PJ, et al. (2011). Expansion of a unique $CD57^{+}$NKG2Chi natural killer cell subset during acute human cytomegalovirus infection. Proc. Natl. Acad. Sci. USA 108, 14725–14732. [PubMed: 21825173]

Ma Y, Li X, and Kuang E (2016). Viral evasion of natural killer cell activation. Viruses 8, 95. [PubMed: 27077876]

Majewska-Szczepanik M, Paust S, von Andrian UH, Askenase PW, and Szczepanik M (2013). Natural killer cell-mediated contact sensitivity develops rapidly and depends on interferon-α, interferon-γ and interleukin-12. Immunology 140, 98–110. [PubMed: 23659714]

Mora JR, Bono MR, Manjunath N, Weninger W, Cavanagh LL, Rosemblatt M, and Von Andrian UH (2003). Selective imprinting of gut-homing T cells by Peyer's patch dendritic cells. Nature 424, 88–93. [PubMed: 12840763]

Nelson CS, Cruz DV, Tran D, Bialas KM, Stamper L, Wu H, Gilbert M, Blair R, Alvarez X, Itell H, et al. (2017). Preexisting antibodies can protect against congenital cytomegalovirus infection in monkeys. JCI Insight 2, 94002. [PubMed: 28679960]

O'Leary JG, Goodarzi M, Drayton DL, and von Andrian UH (2006). T cell- and B cell-independent adaptive immunity mediated by natural killer cells. Nat. Immunol 7, 507–516. [PubMed: 16617337]

O'Shea JJ, Weissman AM, Kennedy IC, and Ortaldo JR. (1991). Engagement of the natural killer cell IgG Fc receptor results in tyrosine phosphorylation of the zeta chain. Proc. Natl. Acad. Sci. USA 88, 350–354. [PubMed: 1703295]

Parsons MS, Wren L, Isitman G, Navis M, Stratov I, Bernard NF, and Kent SJ (2012). HIV infection abrogates the functional advantage of natural killer cells educated through KIR3DL1/HLA-Bw4 interactions to mediate anti-HIV antibody-dependent cellular cytotoxicity. J. Virol 86, 4488–4495. [PubMed: 22345455]

Paust S, Gill HS, Wang BZ, Flynn MP, Moseman EA, Senman B, Szczepanik M, Telenti A, Askenase PW, Compans RW, and von Andrian UH. (2010). Critical role for the chemokine receptor CXCR6 in NK cell-mediated antigen-specific memory of haptens and viruses. Nat. Immunol 11, 1127–1135. [PubMed: 20972432]

Paust S, Blish CA, and Reeves RK (2017). Redefining memory: building the case for adaptive NK cells. J. Virol 91, e00169–17. [PubMed: 28794018]

Reeves RK, Evans TI, Gillis J, and Johnson RP. (2010a). Simian immunodeficiency virus infection induces expansion of alpha4beta7+ and cytotoxic CD56+ NK cells. J. Virol 84, 8959–8963. [PubMed: 20554780]

Reeves RK, Gillis J, Wong FE, Yu Y, Connole M, and Johnson RP (2010b). CD16- natural killer cells: enrichment in mucosal and secondary lymphoid tissues and altered function during chronic SIV infection. Blood 115, 4439–4446. [PubMed: 20339088]

Reeves RK, Li H, Jost S, Blass E, Li H, Schafer JL, Varner V, Manickam C, Eslamizar L, Altfeld M, et al. (2015). Antigen-specific NK cell memory in rhesus macaques. Nat. Immunol 16, 927–932. [PubMed: 26193080]

Robbins SH, Tessmer MS, Mikayama T, and Brossay L (2004). Expansion and contraction of the NK cell compartment in response to murine cytomegalovirus infection. J. Immunol 173, 259–266. [PubMed: 15210783]

Romee R, Foley B, Lenvik T, Wang Y, Zhang B, Ankarlo D, Luo X, Cooley S, Verneris M, Walcheck B, and Miller J (2013). NK cell CD16 surface expression and function is regulated by a disintegrin and metalloprotease-17 (ADAM17). Blood 121, 3599–3608. [PubMed: 23487023]

Schafer JL, Li H, Evans TI, Estes JD, and Reeves RK (2015). Accumulation of cytotoxic CD16+ NK cells in simian immunodeficiency virus-infected lymph nodes associated with in situ differentiation and functional anergy. J. Virol 89, 6887–6894. [PubMed: 25903330]

Schlums H, Cichocki F, Tesi B, Theorell J, Béziat V, Holmes TD, Han H, Chiang SC, Foley B, Mattsson K, et al. (2015). Cytomegalovirus infection drives adaptive epigenetic diversification of NK cells with altered signaling and effector function. Immunity 42, 443–456. [PubMed: 25786176]

Shang L, Smith AJ, Duan L, Perkey KE, Qu L, Wietgrefe S, Zupancic M, Southern PJ, Masek-Hammerman K, Reeves RK, et al. (2014). NK cell responses to simian immunodeficiency virus vaginal exposure in naive and vaccinated rhesus macaques. J. Immunol 193, 277–284. [PubMed: 24899503]

Strauss-Albee DM, Fukuyama J, Liang EC, Yao Y, Jarrell JA, Drake AL, Kinuthia J, Montgomery RR, John-Stewart G, Holmes S, and Blish CA (2015). Human NK cell repertoire diversity reflects immune experience and correlates with viral susceptibility. Sci. Transl. Med 7, 297ra115.

Sun JC, Beilke JN, and Lanier LL (2009). Adaptive immune features of natural killer cells. Nature 457, 557–561. [PubMed: 19136945]

Takahashi Y, Byrareddy SN, Albrecht C, Brameier M, Walter L, Mayne AE, Dunbar P, Russo R, Little DM, Villinger T, et al. (2014). Invivo administration of a JAK3 inhibitor during acute SIV infection leads to significant increases in viral load during chronic infection. PLoS Pathog 10, e1003929. [PubMed: 24603870]

Vivier E, Morin P, O'Brien C, Druker B, Schlossman SF, and Anderson P (1991a). Tyrosine phosphorylation of the Fc gamma RIII(CD16): zeta complexin human natural killer cells.

Induction by antibody-dependent cytotoxicity but not by natural killing. J. Immunol 146, 206–210. [PubMed: 1701792]

Vivier E, Rochet N, Kochan JP, Presky DH, Schlossman SF, and Anderson P (1991b). Structural similarity between Fc receptors and T cell receptors. Expression of the gamma-subunit of Fc epsilon RI in human T cells, natural killer cells and thymocytes. J. Immunol 147, 4263–4270. [PubMed: 1836482]

Vivier E, Rochet N, Ackerly M, Petrini J, Levine H, Daley J, and Anderson P (1992). Signaling function of reconstituted CD16: zeta: gamma receptor complex isoforms. Int. Immunol 4, 1313–1323. [PubMed: 1472481]

Ward J, Bonaparte M, Sacks J, Guterman J, Fogli M, Mavilio D, and Barker E (2007). HIV modulates the expression of ligands important in triggering natural killer cell cytotoxic responses on infected primary T-cell blasts. Blood 110, 1207–1214. [PubMed: 17513617]

Whitney JB, Hill AL, Sanisetty S, Penaloza-MacMaster P, Liu J, Shetty M, Parenteau L, Cabral C, Shields J, Blackmore S, et al. (2014). Rapid seeding of the viral reservoir prior to SIV viraemia in rhesus monkeys. Nature 512, 74–77. [PubMed: 25042999]

Wirthmueller U, Kurosaki T, Murakami MS, and Ravetch JV (1992). Signal transduction by Fc gamma RIII (CD16) is mediated through the gamma chain. J. Exp. Med 175, 1381–1390. [PubMed: 1314888]

Wren LH, Chung AW, Isitman G, Kelleher AD, Parsons MS, Amin J, Cooper DA, ADCC study collaboration investigators,; Stratov I, Navis M, et al. (2013). Specific antibody-dependent cellular cytotoxicity responses associated with slow progression of HIV infection. Immunology 138,116–123. [PubMed: 23173935]

Zhou J, Amran FS, Kramski M, Angelovich TA, Elliott J, Hearps AC, Price P, and Jaworowski A (2015). An NK cell population lacking FcRγ is expanded in chronically infected HIV patients. J. Immunol 194, 4688–4697. [PubMed: 25855354]

Highlights

- Δg NK cell expansion and acquisition of function are driven by concurrent CMV infection
- Δg NK cells are distributed systemically but have the propensity to migrate to mucosal sites
- Δg NK cells abandon γ-chain/Syk signaling in lieu of the atypical CD3ζ-Zap70 signaling pathway
- SIV infection subverts Δg NK cells by suppressing CD16-mediated CD3ζ-ZAP70 signaling

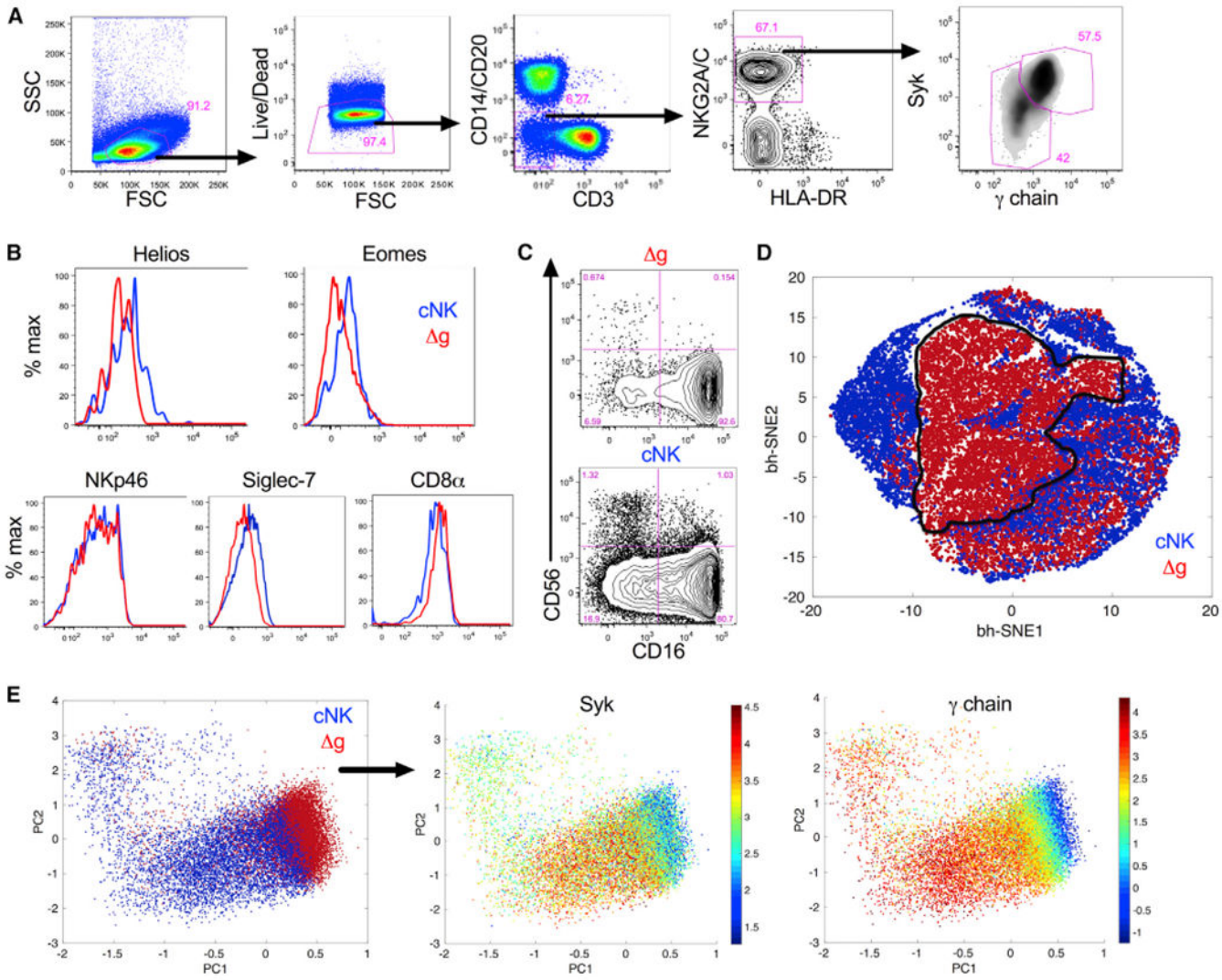

Figure 1. Identification of a Distinct Population of γ-chain/Syk-Deficient NK Cells in rhCMV+ Rhesus Macaques

(A) Representative gating strategy identifying Δg among bulk NK cells.

(B) Representative histograms showing expression of NKp46, CD8α, Siglec-7, Helios, and Eomes in Δg and cNK cells.

(C) Representative flow cytometry plots indicating distribution of $CD56^{+}$ and $CD16^{+}$ subpopulations in Δg and cNK cells.

(D and E) Composite phenotypic *t*-SNE plot (D) and PCA analysis (E) of bulk NK cells down-selected from rhCMV-infected rhesus macaque cohorts showing independent multidimensional clustering of Δg NK cells; data points represent individual cells. Individual parameters are shown in Figure S3. All plots are representative of 6 to 70 animals depending on grouping and measured parameter.

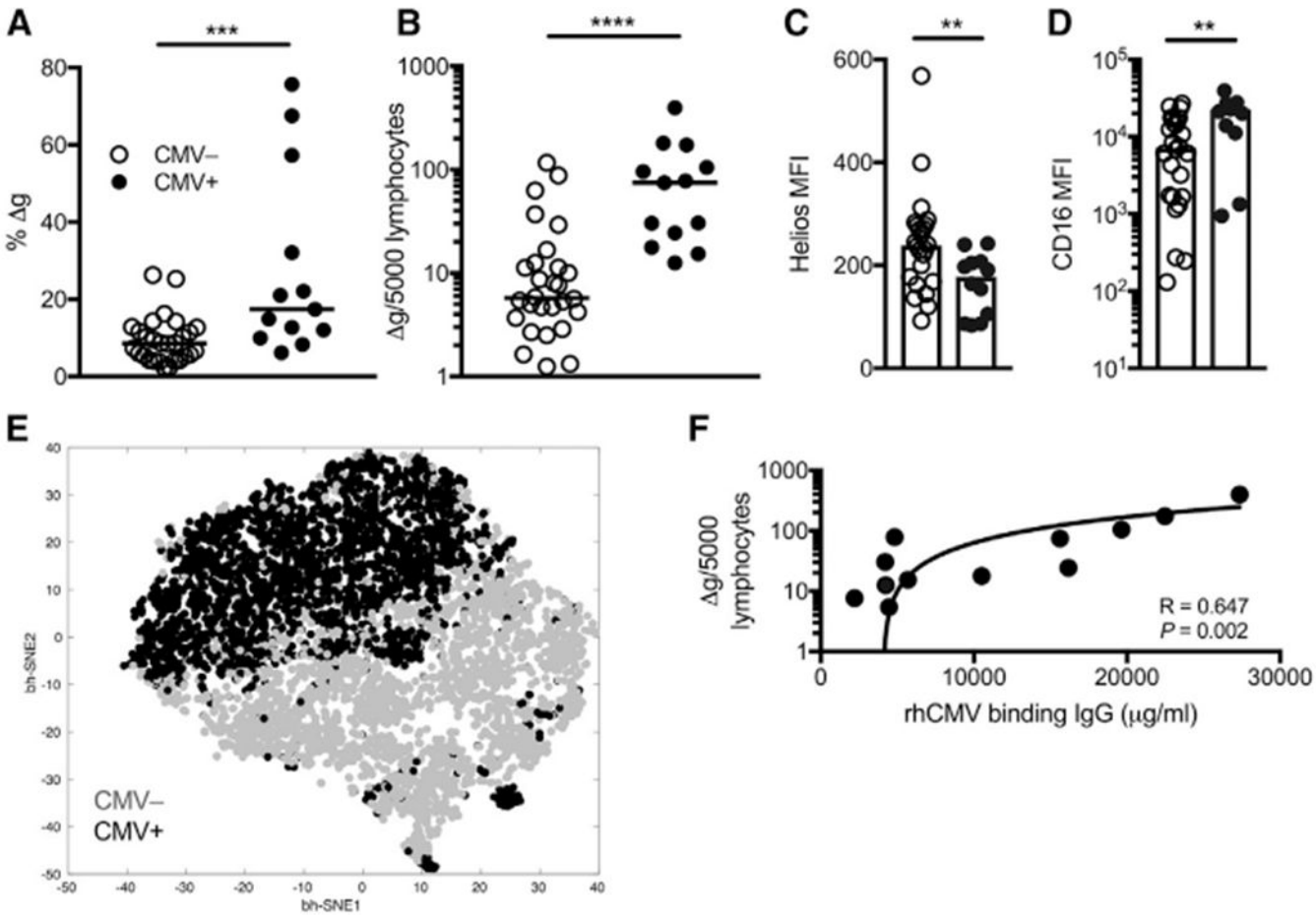

Figure 2. Δg NK Cells Are Primed by CMV Status

(A–D) Frequencies among bulk NK cells (A) and normalized circulating numbers of Δg NK cells (B) are shown for rhCMV-uninfected (n = 28) and rhCMV-infected (n = 14) rhesus macaques. Horizontal lines indicate medians. Density of intracellular Helios (MFI, median fluorescence intensity) (C) and surface CD16 on Δg NK cells (D) in peripheral blood nuclear cells (PBMCs) from rhCMV-uninfected and rhCMV-infected macaques. Bars indicate medians.

(E) Composite phenotypic *t*-SNE plot of Δg NK cells only down-selected in both rhCMV-uninfected and rhCMV-infected rhesus macaque cohorts showing near complete independent multidimensional clustering by rhCMV-specific IgG levels; data points represent individual cells.

(F) Correlation of circulating Δg NK cell numbers with rhCMV-binding antibody equivalents.

Statistical evaluations were made with Mann Whitney *U* or Spearman's correlation test; **p <0.01; ***p < 0.001; ****p < 0.0001.

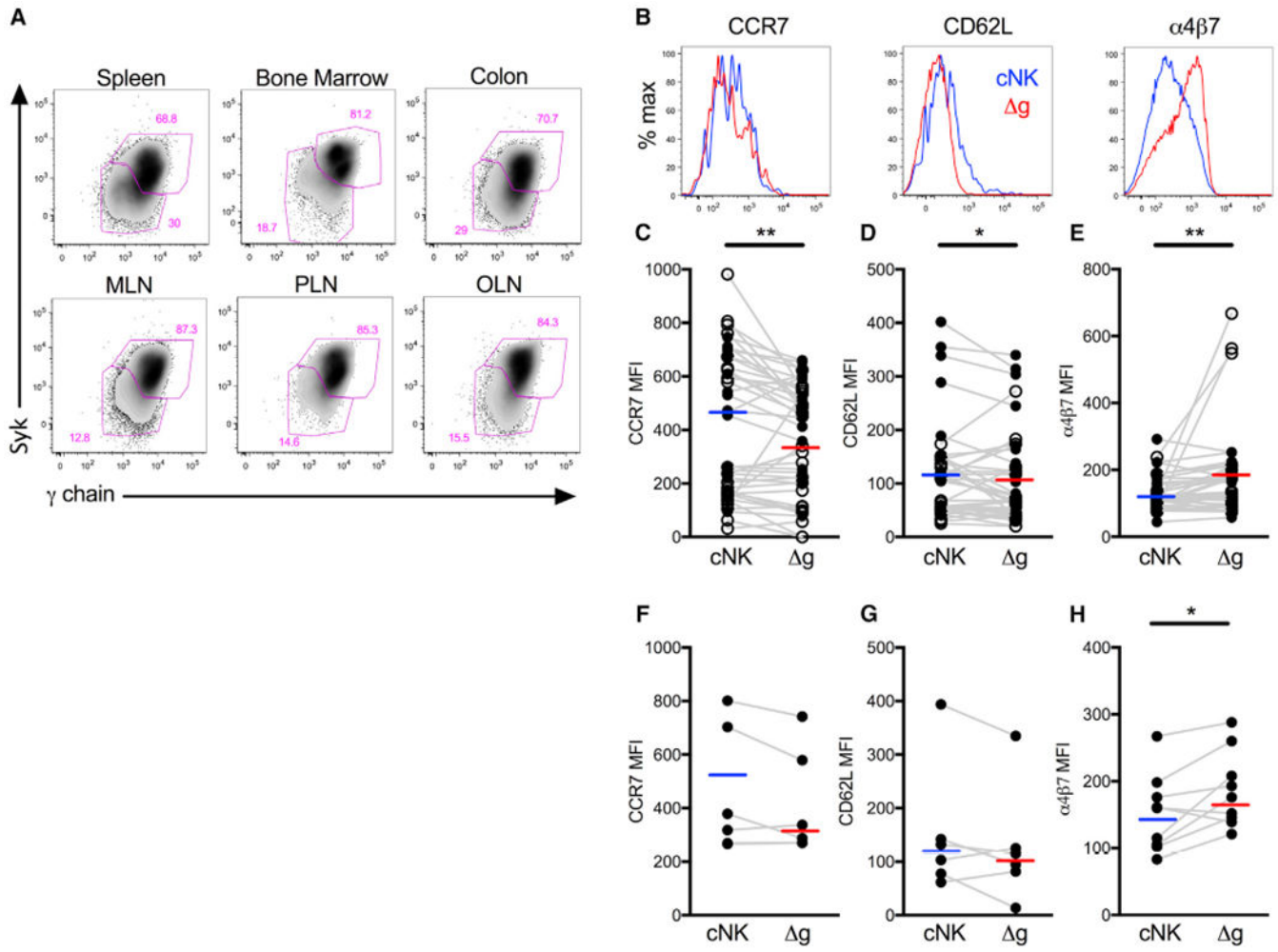

Figure 3. Systemic Distribution and Mucosal-Homing of Δg NK Cells

(A) Representative flow cytometry plots showing Δg NK cells in secondary lymphoid and colonic tissues.

(B) Representative histograms showing CCR7, CD62L, and α4β7 expression on Δg and cNK cells in PBMC.

(C–H) Median fluorescence intensities (MFI) of CCR7 (C), CD62L(D), and α4β7 (E) on Δg and cNK cells in PBMC from rhCMV-uninfected (n = 28, open circles) and rhCMV-infected (n = 14, closed circles) rhesus macaques. MFI of CCR7 (F) and CD62L (G) on LN resident NK cells, and α4β7 (H) on colonic NK cells. Horizontal lines indicate medians, and connecting lines are shown between individual animals.

Statistical evaluations were made with Wilcoxon rank-sum test; *p < 0.05; **p < 0.01.

MLN, mesenteric lymph node; PLN, peripheral lymph node; OLN, oral lymph nodes.

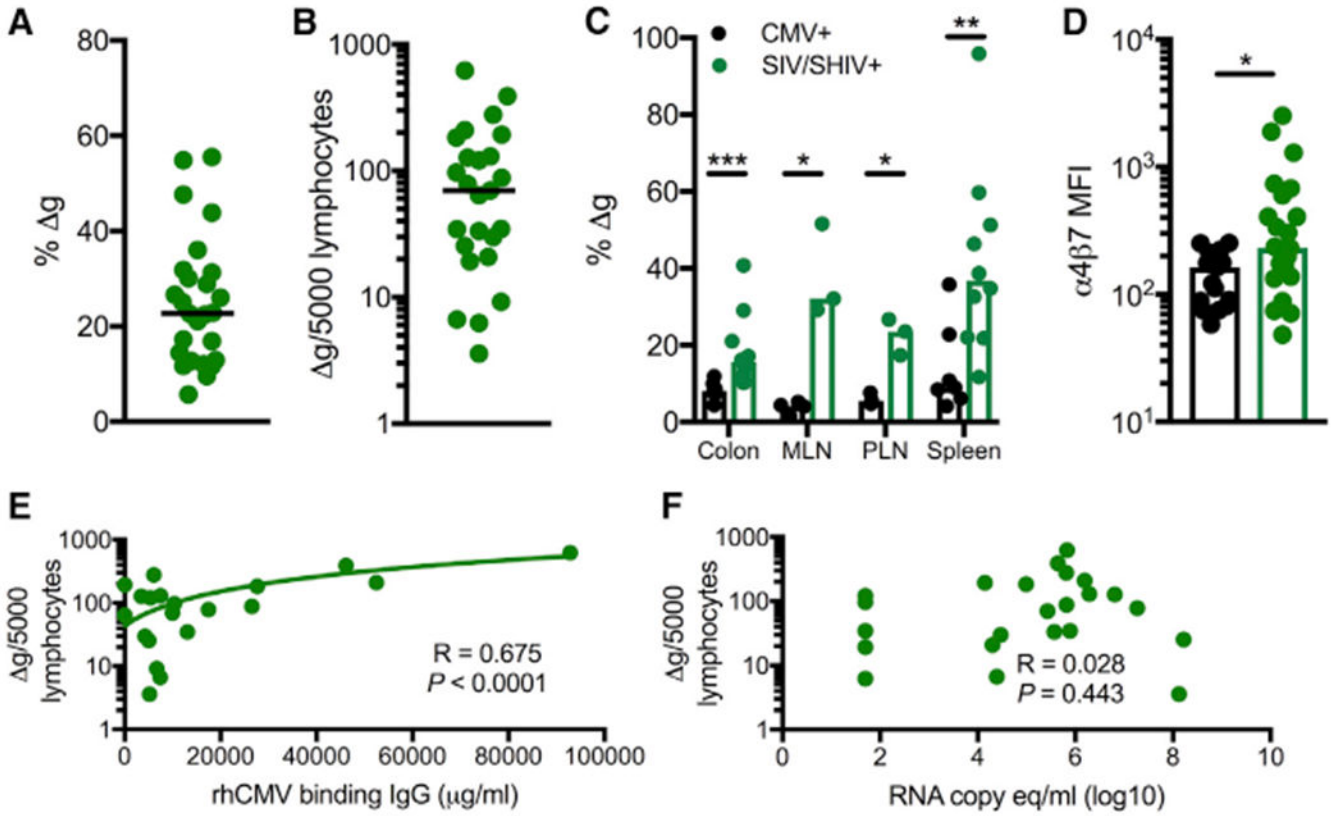

Figure 4. Mucosal-Homing Δg NK Cells Expand during SIVmac251/SHIV162p3 Infection

(A) Frequencies among bulk NK cells in SIVmac251/SHIV162p3-infected rhesus macaques (n = 28). Horizontal bars indicate medians.

(B) Frequencies among normalized circulating numbers of Δg NK cells in SIVmac251/SHIV162p3-infected rhesus macaques (n = 28). Horizontal bars indicate medians.

(C) Frequencies of Δg NK cells among tissue mononuclear r cells in of SIV and SHIV-infected (also rhCMV-infected) and otherwise normal rhCMV-infected macaques. Bars indicate medians.

(D) Density of surface α4β7 (MFI, median fluorescence intensity) on Δg NK cells in PBMC.

(E and F) Correlations of Δg NK cell numbers with rhCMV-binding antibody equivalents (E) and SIVmac251/SHIV162p3 plasma virus loads (F).

Statistical evaluations were made with Mann Whitney *U* or Spearman's correlation test; *p < 0.05; **p < 0.01; ***p < 0.001.

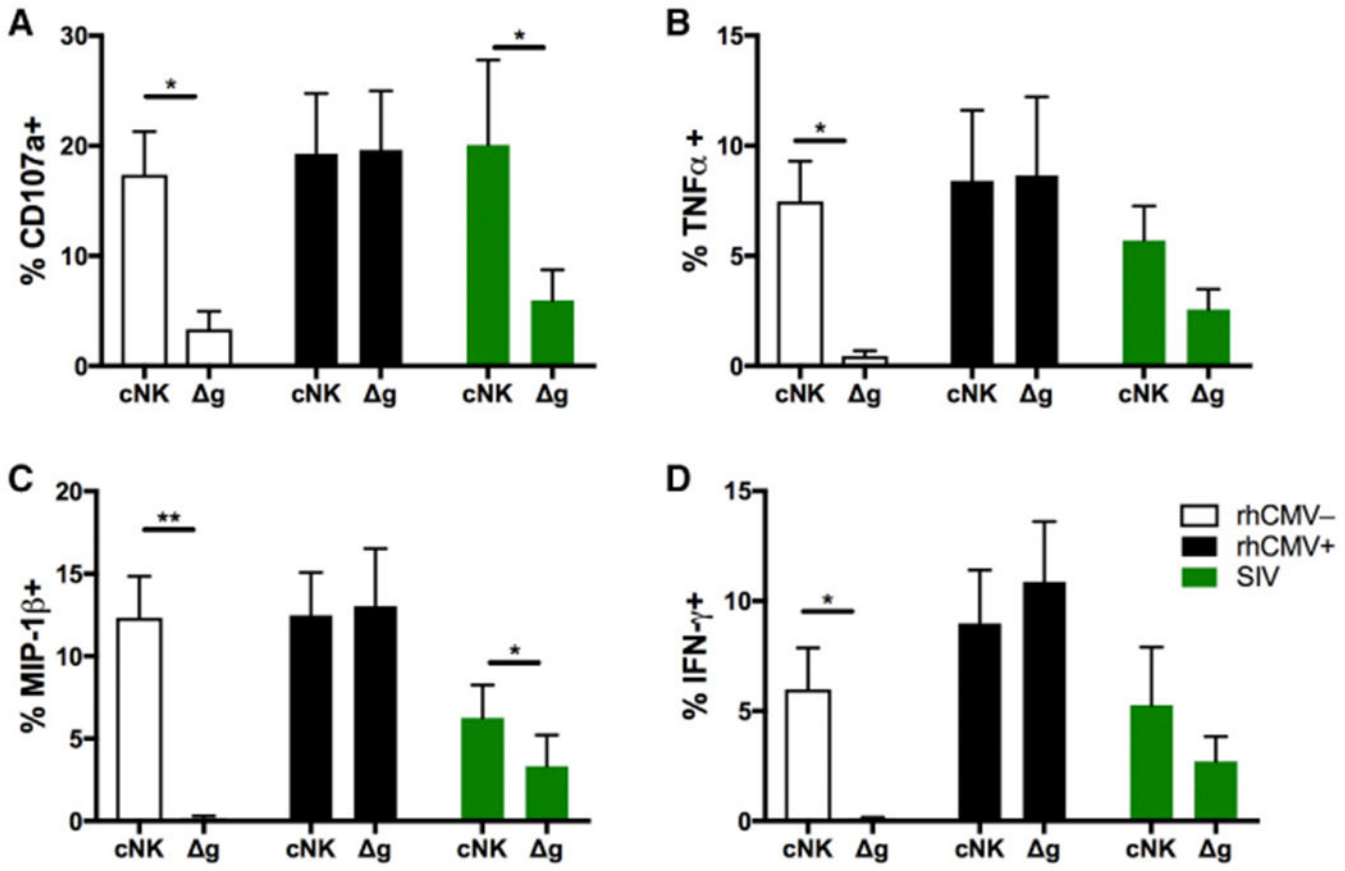

Figure 5. Functional Differences in cNK and Δg NK Cells in rhCMV-Uninfected, rhCMV-Infected, and SIVmac251/SHIV162p3-Infected Rhesus Macaques

(A–D) Intracellular expression of CD107a (A) and production of TNF-α (B), MIP-1β (C), and IFN-γ (D) were measured by ADCC ICS as described in the STAR Methods.

Bars represent means ± SEM of 6–8 animal samples per group. Statistical comparisons between Δg and cNK cells were conducted using Student's paired t test; *$p < 0.05$; **$p < 0.01$.

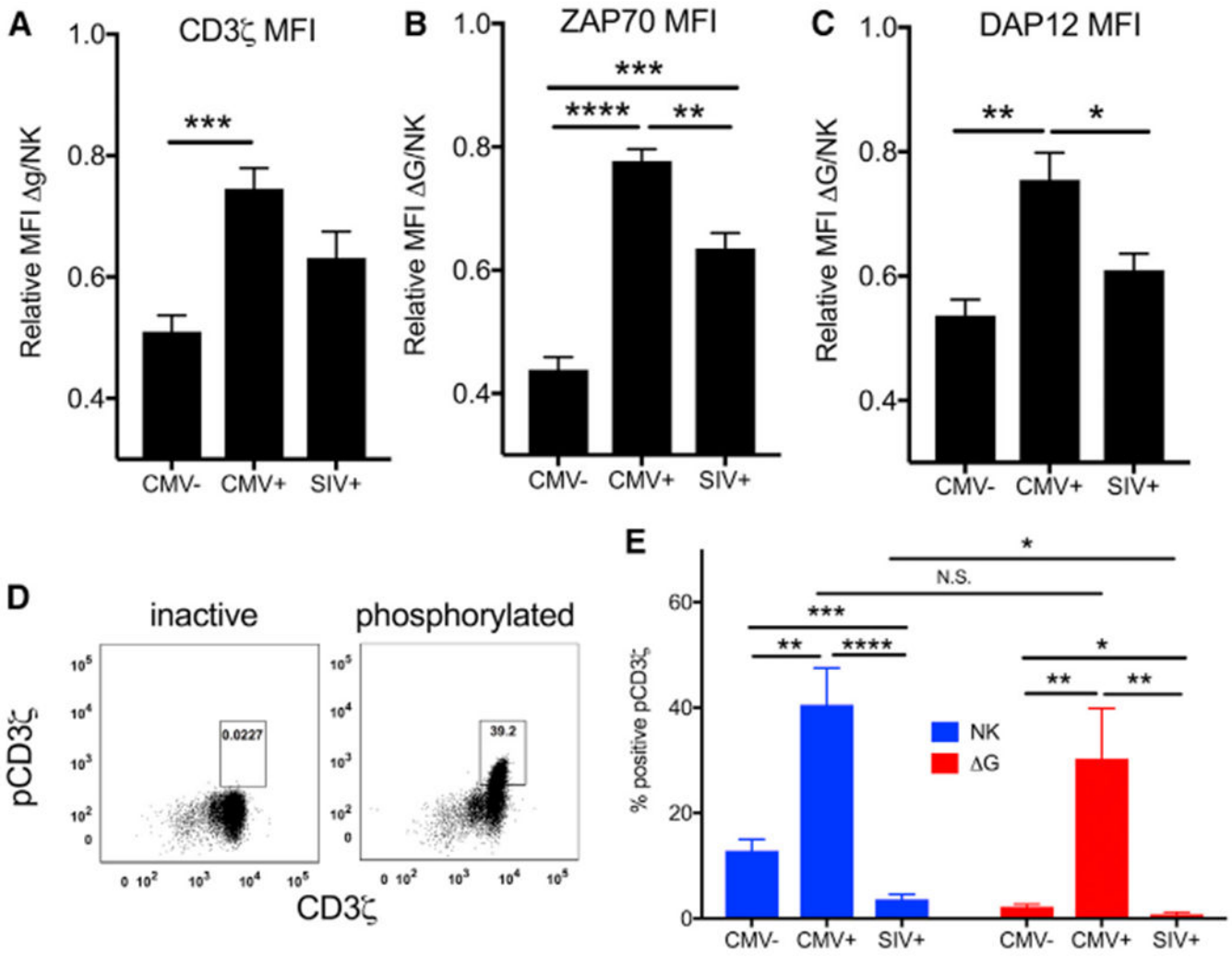

Figure 6. cNK and Δg NK Cell Signaling in rhCMV-Uninfected, rhCMV-Infected, and SIVmac251/SHIV162p3-Infected Rhesus Macaques

(A–C) Expression of signaling molecules involved in the CD16 signaling pathway were measured by intracellular and phosphor-flow cytometry. Relative expression of parent signaling molecules CD3ζ (A), ZAP70 (B), and DAP12 (C) in Δg NK cells relative to expression in cNK cells.

(D) Representative plots from inactive and activated phosphoCD3ζ samples are shown. Δg and cNK cells were gated as shown in Figure 1.

(E) Frequencies of phosphorylated parent CD3ζ are shown as bars representing means ± SEM of 6–10 animal samples per group.

Statistical comparisons between infection groups were conducted with the Mann-Whitney *U* test, and statistical comparisons between conditions for individual animals were conducted using Wilcoxon rank-sum test; *p < 0.05; **p < 0.01; ***p <0.001, ****p<0.0001.

KEY RESOURCES TABLE

REAGENT or RESOURCE	SOURCE	IDENTIFIER
Antibodies (clone)		
α4β7-APC (A4B7)	http://nhpreagents.org/NHP/default.aspx	Cat# PR-1421
CD3-BV786 (SP34.2)	3D Biosciences	Cat# 563918; RRID: AB_2738487
CD8-BV650 (RPA-T8)	3D Biosciences	Cat# 563822; RRID: AB_2744462
CD8-BV605 (SK1)	BD Biosciences	Cat# 564116; RRID: AB_2744466
CD14-BUV395 (MϕP9)	BD Biosciences	Cat# 563561; RRID: AB_2744288
CD16-BUV496 (3G8)	BD Biosciences	Cat# 564653; RRID: AB_2744294
CD20-BUV395 (L27)	BD Biosciences	Cat# 740204; RRID: AB_2739954
CD56-BV786 (NCAM16.2)	BD Biosciences	Cat# 564058; RRID: AB_2738569
CD62L-BV711 (SK11)	BD Biosciences	Cat# 565040; RRID: AB_2744438
CD69-ECD (TP1.55.3)	Beckman Coulter	Cat# 6607110; RRID: AB_1575978
CD95/Fas-BUV737 (DX2)	BD Biosciences	Cat# 564710; RRID: AB_2738907
CD95/Fas-APC (DX2)	BD Biosciences	Cat# 558814; RRID: AB_398659
CD107a/LAMP-1-PECF594 (H4A3)	BD Biosciences	Cat# 562628; RRID: AB_2737686
CD107a/LAMP-1-PE-Cy7 (H4A3)	BD Biosciences	Cat# 561348; RRID: AB_10644018
CD159a/NKG2a-APC (Z199)	Beckman Coulter	Cat# A60797; RRID: AB_10643105
CD159a/NKG2a-PC7 (Z199)	Beckman Coulter	Cat# B10246; RRID: AB_2687887
CD197/CCR7-BV421 (G043H7)	BioLegend	Cat# 353208; RRID: AB_11203894
CD247/CD3ζ-FITC (H146-968)	ThermoFisher Scientific	Cat# MA5-17673; RRID: AB_2539063
CD328/Siglec-7-PerCP-Vio700 (REA214)	MILTENYI	Cat# 130-100-979; RRID: AB_2657543
CD335/NKp46-PC5 (BAB281)	Beckman Coulter	Cat# A66904
CD335/NKp46-PC7 (BAB281)	Beckman Coulter	Cat# B38703
CD335/NKp46-PE (BAB281)	Beckman Coulter	Cat# IM3711; RRID: AB_1575960
CD337/NKp30-BV605 (p30-15)	BD Biosciences	Cat# 563384; RRID: AB_2738170
DAP12-Alexa Fluor488 (406288)	NOVUS BIOLOGICALS	Cat# IC5240G
EOMES-PerCP-eFluor710 (WD1928)	ThermoFisher Scientific	Cat# 46-4877-42; RRID: AB_2573759
FcR (γ-chain)-FITC (rabbit polyclonal)	Millipore Milli-Mark	Cat# FCABS400F; RRID: AB_11203492
FcR (γ-chain)-Alexa Fluor700 (rabbit polyclonal)	Millipore Milli-Mark	Conjugated in-house
Granzyme B-Alexa Fluor700 (GB11)	BD Biosciences	Cat# 560213; RRID: AB_1645453

REAGENT or RESOURCE	SOURCE	IDENTIFIER
HELIOS-e450 (22F6)	ThermoFisher Scientific	Cat# 48-9883-42; RRID: AB_2574136
HELIOS-PE E610 (22F6)	ThermoFisher Scientific	Cat# 61-9883-42; RRID: AB_2574682
HLA-DR-ECD (HLA-DR)	Beckman Coulter	Cat# IM3636; RRID: AB_10643231
IFN-γ-PE-Cy7 (B27)	BD Biosciences	Cat# 560924; RRID: AB_2033978
IFN-γ-BV711 (B27)	BD Biosciences	Cat# 564039; RRID: AB_2738557
MIP1-β-APC-H7 (D21-1351)	BD Biosciences	Cat# 561280; RRID: AB_10611567
Perforin-FITC (pf344)	mABTech	Cat# 3465-7; RRID: AB_1925742
Perforin-Pacific Blue (dG9)	BioLegend	Cat# 308118; RRID: AB_10899565
phospho-CD3ζ-Alexa Fluor647 (K25-407.69)	BD Biosciences	Cat# 558489; RRID: AB_647152
phospho-Syk-Pacific Blue (rabbit polyclonal)	Cell Signaling Technology	Cat# 12967
phospho-Syk/ZAP70-PE-Cy7 (17A/P-ZAP70)	BD Biosciences	Cat# 561458; RRID: AB_10696417
Syk-PE (4D10.1)	ThermoFisher Scientific	Cat# 17-6696-42; RRID: AB_10714836
TNF-α-BV650 (Mab11)	BD Biosciences	Cat# 563418; RRID: AB_2738194
ZAP70-Pacific Blue (1E7.2)	ThermoFisher Scientific	Cat# MHZAP7004-4; RRID: AB_2539777
Critical Commercial Reagents		
Fix Buffer I phosflow™	BD Biosciences	Cat# 557870
Perm Buffer III phosflow™	BD Biosciences	Cat# 558050
Fixation Medium A	ThermoFisher Scientific	Cat# GAS001S100
Permeabilization Medium B	ThermoFisher Scientific	Cat# GAS002S100
Experimental Models: Organisms		
Macaca mulatta	Tulane National Primate Research Center	N/A
Macaca mulatta	Alphagenesis Inc.	N/A
Software		
Graphpad Prism 7	GraphPad Software	https://www.graphpad.com/scientific-software/prism/
FacsDiva	BD Biosciences	http://www.bdbiosciences.com/us/instruments/clinical/software/flowcytometry-acquisition/bd-facsdiva-software/m/333333/overview
FlowJo	FlowJo LLC	https://www.flowjo.com/solutions/flowio/downloads